CRYSTALLOGRAPHIC
COMMUNICATIONS

ISSN 2056-9890

Synthesis, crystal structure and thermal properties of di-μ-iodido-bis[bis(2-chloropyrazine-κN)-copper(I)]

Christian Näther* and Inke Jess

Institut für Anorganische Chemie, Universität Kiel, Max-Eyth.-Str. 2, 24118 Kiel, Germany. *Correspondence e-mail: cnaether@ac.uni-kiel.de

Received 16 January 2023
Accepted 10 February 2023

Edited by V. Jancik, Universidad Nacional Autónoma de México, México

Keywords: synthesis; crystal structure; binuclear complex; thermal properties.

CCDC reference: 2241117

Supporting information: this article has supporting information at journals.iucr.org/e

Reaction of copper(I) iodide in pure 2-chloropyrazine leads to the formation of a few crystals of the title compound, $[Cu_2I_2(C_4H_3ClN_2)_4]$ or $(CuI)_2$(2-chloropyrazine)$_4$, which was characterized by single-crystal X-ray diffraction. In its crystal structure, the Cu^I cations are each tetrahedrally coordinated by two iodide anions and two 2-chloropyrazine ligands and are linked into binuclear complexes consisting of $(CuI)_2$ rings located on centers of inversion. PXRD investigations of a few crystals obtained from the suspension indicate that the title compound is contaminated with a small amount of the 2-chloropyrazine-deficient compound CuI(2-chloropyrazine) already reported in the literature. PXRD investigations prove that the title compound immediately decomposes at room temperature into CuI(2-chloropyrazine) and this might be the reason why no pure samples can be obtained. TDA–TG–MS investigations shows two mass losses, the first of which corresponds to the formation of CuI(2-chloropyrazine), whereas in the second mass loss CuI is formed.

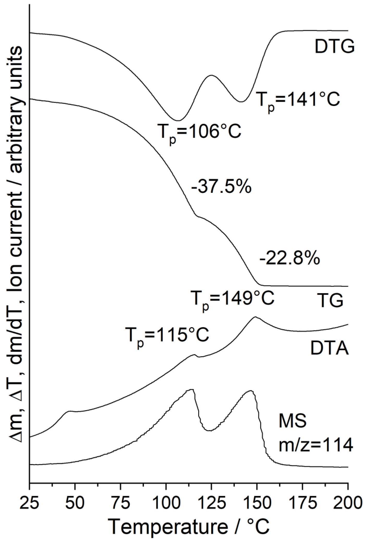

1. Chemical context

Coordination compounds based on transition-metal halides show a versatile structural behavior, which is observed particularly in compounds that contain Cu^I cations (Kromp & Sheldrick, 1999; Peng *et al.*, 2010; Li *et al.*, 2005; Näther & Jess, 2004). These compounds are also of interest because of their luminescence behavior (Gibbons *et al.*, 2017; Mensah *et al.*, 2022). For one given metal halide CuX (X = Cl, Br, I) and one specific neutral coligand, several compounds are usually observed that differ in the ratio between the metal halide and the coligand – this is the reason why so many compounds with different CuX (X = Cl, Br, I) substructures (such as, for example, dimers, single and double chains or layers) are observed that can be further connected into more condensed networks if bridging neutral coligands are used in the synthesis. In general, it is observed that with decreasing amounts of the coligand, the synthesis leads to the formation of compounds with more condensed CuX substructures. In this context, it is noted that upon heating, the most coligand-rich compounds usually lose their coligands stepwise and transform into coligand-deficient phases and that this is not limited to Cu^I, but can also be expanded to Cd^{II} and Zn^{II} compounds (Näther *et al.*, 2001, 2007, 2017; Näther & Jess, 2001). This can easily be investigated by thermogravimetry of the most coligand-rich compounds, where each mass loss corresponds to the formation of a new coligand-deficient phase with a more condensed CuX substructure. Surprisingly, even for

https://doi.org/10.1107/S2056989023001238

compounds with the same CuX:ligand ratio, sometimes a different thermal reactivity is observed. This is the case, for example, for compounds based on CuX (X = Cl, Br, I) and 2-chloropyrazine as ligands with the general composition CuX(2-chloropyrazine) (X = Cl, Br, I; Näther, Wriedt & Jess, 2002; Näther, Greve & Jess, 2002). In the isotypic chloride and bromide compounds, the copper cations are tetrahedrally coordinated by two bridging 2-chloropyrazine ligands and two halide anions. The cations are linked by single μ-1,1-bridging halide anions into chains that are further connected into layers by μ-1,4-bridging 2-chloropyrazine ligands (Fig. S1 in the supporting information). In contrast, in CuI(2-chloropyrazine), each copper cation is tetrahedrally coordinated by three iodide anions and only one terminal N-bonding 2-chloropyrazine ligand that is coordinated to the copper center by the N atom that is not adjacent to the chloro substituent. The cations are linked into double chains *via* bridging iodide anions (Fig. S1). If the chloride and the bromide compounds are heated, all 2-chloropyrazine ligands are removed in a single step, leading to the formation of CuX (X = Cl, Br). In contrast, the iodide compound decomposes in two discrete steps, where in the first step only half of the coligands are removed, leading to the formation of $(CuI)_2$(2-chloropyrazine), which decomposes into CuI upon further heating (Näther, Greve & Jess, 2002).

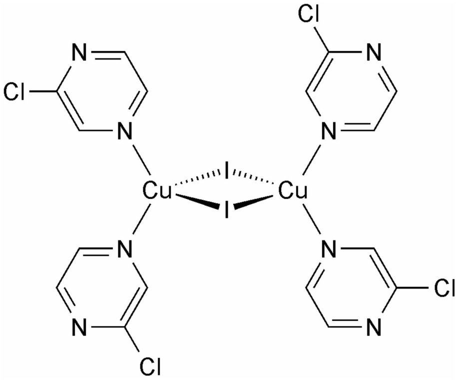

Concerning the composition of all of these compounds, in principle, more 2-chloropyrazine-rich compounds with the composition CuX(2-chloropyrazine)$_2$ might exist, in which, according to simple chemical considerations, each two copper cations would be tetrahedrally coordinated by two halide anions and two N-terminal 2-chloropyrazine ligands and linked into binuclear complexes by pairs of μ-1,1-bridging halide anions. One might argue that this arrangement is less stable compared to that with bridging 2-chloropyrazine ligands, but one should keep in mind that both N atoms of this ligand are not equivalent, because coordination to the N atom that is adjacent to the chloro substituent is sterically hindered. That this coordination exists is obvious from the crystal structure of (CuI)(2-chloropyrazine) mentioned above, even if this CuX substructure is different. Moreover, a few compounds with such a structure have already been reported in the literature, including, for example, $(CuI)_2$(2-cyanopyrazine)$_4$ (Refcodes: DINQIA and DINQIA01; Rossenbeck & Sheldrick, 1999 and Jana *et al.*, 2016), $(CuI)_2$(2-ethylpyrazine)$_4$ (Refcode: EMELEN; Näther *et al.*, 2003), $(CuI)_2$(methylsulfanylpyrazine)$_4$ (Refcode: QOWYOT; Artem'ev *et al.*, 2019) and $(CuI)_2$(2,2′-biquinoxaline) (Refcode: RIXGEL; Fitchett & Steel, 2008), all with iodide as counter-anion.

To check if such a compound can be synthesized, all three copper(I) halides were reacted in different solvents with a very large excess of 2-chloropyrazine, but no new crystalline phases were observed. On the contrary, if CuI is reacted as a suspension in pure 2-chloropyrazine, yellow-colored crystals of a new crystalline phase are obtained. In contrast, with CuCl or CuBr only the known compounds CuX(2-chloropyrazine) with X = Cl, Br are obtained. Single-crystal structure analysis proved that a new compound with the composition $(CuI)_2$(2-chloropyrazine)$_4$ has been obtained.

2. Structural commentary

The asymmetric unit of the title compound $(CuI)_2$(2-chloropyrazine)$_4$ consists of one copper(I) cation, one iodide anion and two 2-chloropyrazine ligands that are located in general positions. The copper(I) cations are tetrahedrally coordinated by two symmetry-related iodide anions and two crystallographically independent 2-chloropyrazine ligands (Fig. 1). Each two copper(I) cations are linked by pairs of μ-1,1-bridging iodide anions into binuclear complexes consisting of four-membered $(CuI)_2$ rings located on centers of inversion. The Cu—Cu distance within these rings amounts to 2.5643 (10) Å (Table 1). Bond lengths and angles are similar to those in related compounds and show that the tetrahedra are strongly distorted (Table 1).

This structure is similar to those of $(CuI)_2$(2-cyanopyrazine)$_4$ (Rossenbeck & Sheldrick, 1999; Jana *et al.*, 2016),

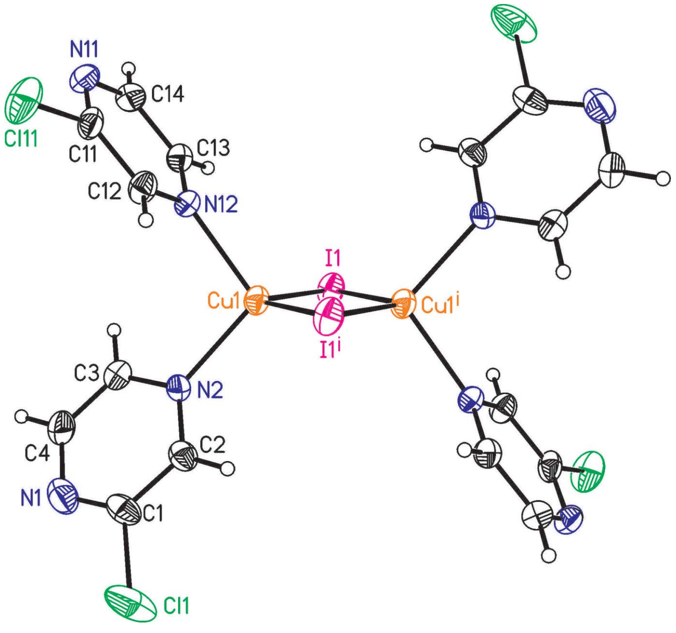

Figure 1
Crystal structure of the title compound with atom labeling and displacement ellipsoids drawn at the 50% probability level. Symmetry codes: (i) $-x + 2, -y + 1, -z + 2$.

Table 1
Selected geometric parameters (Å, °).

Cu1—N2	2.070 (3)	Cu1—I1	2.6093 (5)
Cu1—N12	2.078 (3)	Cu1—I1^{i}	2.6476 (6)
Cu1—Cu1^{i}	2.5643 (10)		
N2—Cu1—N12	103.01 (12)	N2—Cu1—I1^{i}	107.58 (9)
N2—Cu1—I1	109.42 (9)	N12—Cu1—I1^{i}	105.80 (9)
N12—Cu1—I1	107.83 (9)	I1—Cu1—I1^{i}	121.61 (2)

Symmetry code: (i) $-x+2, -y+1, -z+2$.

$(CuI)_2$(2-ethylpyrazine)$_4$ (Näther *et al.*, 2003), $(CuI)_2$(methylsulfanylpyrazine)$_4$ (Artem'ev *et al.*, 2019) and $(CuI)_2$(2,2′-biquinoxaline) (Fitchett & Steel, 2008) already reported in the literature, which also form binuclear complexes with $(CuI)_2$ rings as the main structural motif.

3. Supramolecular features

In the crystal structure of the title compound, the binuclear complexes are arranged in columns that propagate along the crystallographic *a*-axis direction (Fig. 2). No directional intermolecular interactions occur between the complexes. One C—H⋯N and one C—H⋯I contact is observed, but their distances and angles indicate that they do not correspond to significant interactions (Table 2).

4. Powder X-ray diffraction and thermoanalytical investigations

Further investigations prove that the unreacted 2-chloropyrazine cannot be removed by filtration and washing because immediate decomposition is observed. Nevertheless, XRPD investigations reveal that most of the sample consists of crystals of the title compound, even if all of the powder patterns are of very low quality, which can be traced back to the instability of this compound and to the fact that only very small amounts of crystals were obtained and these were embedded in pure 2-chloropyrazine and that grinding of such samples leads to the formation of an amorphous phase (Fig. S2). Careful inspection of the powder pattern indicates that this sample is contaminated at least with CuI(2-chloropyrazine) reported in the literature (Näther, Greve & Jess, 2002). This indicates that the title compound has already decomposed into this compound at room temperature. To prove this assumption, freshly prepared crystals were stored at room temperature overnight and were afterwards investigated by PXRD, confirming that the title compound has been completely transformed into the ligand-deficient compound CuI(2-chloropyrazine) (Fig. S3). These observations indicate that CuI(2-chloropyrazine) with a bridging coordination of the 2-chloropyrazine ligand is more stable than the title compound, in which the 2-chloropyrazine acts as a terminal ligand. Additional DTA–TG–MS investigations reveal that the title compound loses two 2-chloropyrazine ligands in two subsequent steps, in which 2-chloropyrazine is always removed (*m*/*z* = 114, Fig. 3). The experimental mass loss in the first step ($\Delta m_{exp.}$ = 37.5%) is much larger than that expected for the

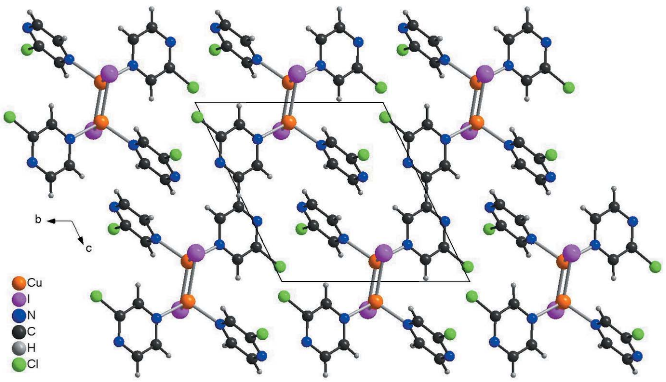

Figure 2
Crystal structure of the title compound in a view along the crystallographic *a*-axis.

Table 2
Hydrogen-bond geometry (Å, °).

D—H⋯*A*	*D*—H	H⋯*A*	*D*⋯*A*	*D*—H⋯*A*
C3—H3⋯N11^{ii}	0.94	2.68	3.241 (5)	119
C13—H13⋯I1	0.94	3.24	3.872 (4)	127

Symmetry code: (ii) $-x+1, -y+1, -z+1$.

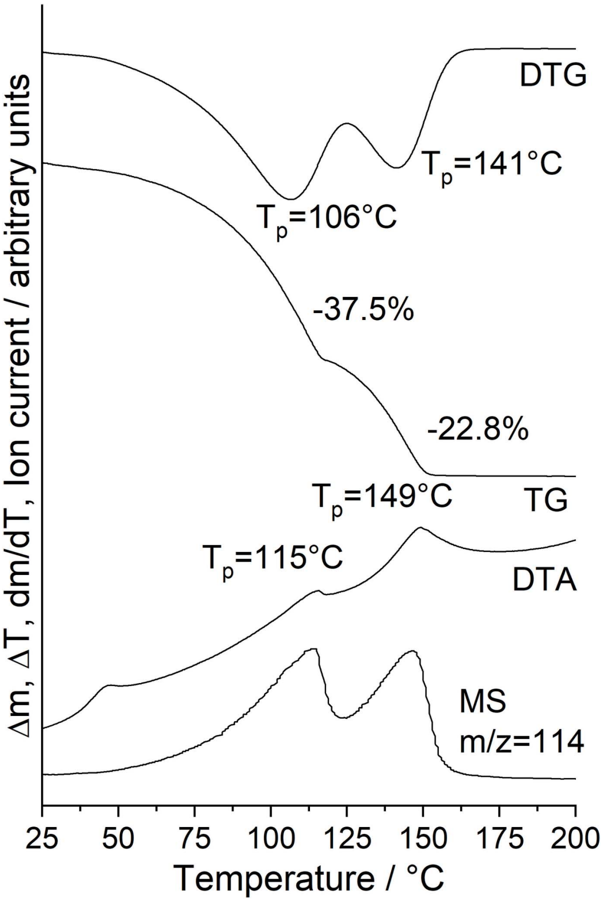

Figure 3
DTG, TG, DTA and MS trend scan curves for the title compound measured with a heating rate of 4°C min^{-1}.

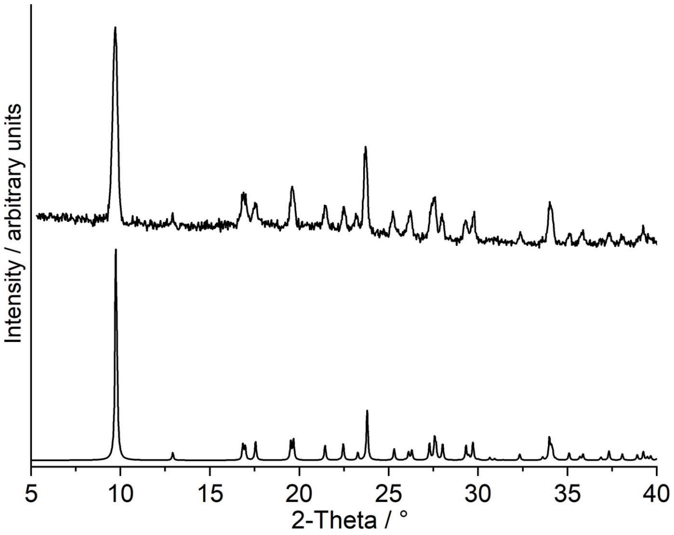

Figure 4
Experimental PXRD pattern of the residue obtained after the first mass loss in a DTA–TG–MS measurement of the title compound (top) and PXRD pattern calculated for CuI(2-chloropyrazine) (bottom).

removal of all of the 2-chloropyrazine ligands from the title compound ($\Delta m_{\rm calc.}$ = 19.1%), which originates from the fact that the 2-chloropyrazine coating the crystals cannot be removed. However, PXRD of the residue obtained after the first mass loss confirms that CuI(2-chloropyrazine) is formed as an intermediate (Fig. 4). It is noted that no additional step is observed that would correspond to the formation of the most 2-chloropyrazine-deficient compound, $(CuI)_2$(2-chloropyrazine), because this event would happen at a much lower temperature, whereas our measurements indicate an excess of 2-chloropyrazine is still present in the gas phase. Finally, the product formed after the second mass loss was also investigated py PXRD, which proves that CuI (Hull, & Keen, 1994) is formed in this step (Fig. S4).

5. Database survey

A search in the CCDC database (Groom *et al.*, 2016, CSD Version 5.43, March 2022) for compounds with a structure similar to that of the title compound revealed several hits, including $(CuI)_2$(2-cyanopyrazine)$_4$ (Refcodes: DINQIA and DINQIA01; Rossenbeck & Sheldrick, 1999; Jana *et al.*, 2016), $(CuI)_2$(2-ethylpyrazine)$_4$ (Refcode: EMELEN; Näther *et al.*, 2003), $(CuI)_2$-(methylsulfanylpyrazine)$_4$ (Refcode: QOWYOT; Artem'ev *et al.*, 2019) and $(CuI)_2$(2,2′-biquinoxaline) (Refcode: RIXGEL; Fitchett & Steel, 2008).

A further search for compounds based on copper halides and 2-chloropyrazine as ligand lead to only a very few compounds. They include the three compounds with the composition CuX(2-chloropyrazine) with X = Cl, Br, I mentioned above (Refcodes: ODOFES, ODOFIW and ODOFOC; Näther, Wriedt & Jess 2002) as well as two isotypic discrete complexes with the composition CuX_2(2-chloropyrazine)$_2$ with X = Cl, Br that contain Cu$^{\rm II}$ cations (Refcodes: FULYIV and FULYOB; Herringer *et al.*, 2010).

Some related compounds can also be found with 2-methylpyrazine as coligand because the exchange of a chloro atom by a methyl group sometimes leads to compounds with similar crystal structures as the van der Waals radius of a chlorine atom is comparable to that of a methyl group (Desiraju & Sarma, 1986). This is obvious from CuX(2-methylpyrazine) with X = Cl, Br (Refcodes: XEBMOG and XEBMIA; Rossenbeck & Sheldrick, 2000), in which the copper(I) cations are linked by μ-1,1-bridging halide anions into chains that are further connected into layers by bridging 2-methylpyrazine ligands. This structure is identical to that of CuX(2-chloropyrazine) (X = Cl, Br). Moreover, both the 2-methylpyrazine and the 2-chloropyrazine compounds crystallize in the monoclinic space group $P2_1/c$ with very similar lengths of the unit-cell axes, but with a significantly different β angle. In this context it is noted that with 2-methylpyrazine, two coligand-deficient compounds with the composition (CuX)$_2$(2-methylpyrazine) with X = Br, I (Refcodes: XEBMUM and XEBNAT; Rossenbeck & Sheldrick, 2000) were observed that could not be prepared with 2-chloropyrazine.

Furthermore, the isotypic compounds (CuX)$_2$(2-methylpyrazine)(triphenylphosphine)$_2$ acetonitrile solvate with X = Br, I [Refcodes: AKOPOI (Kuwahara *et al.*, 2020) and RAYXAT (Liu *et al.*, 2017)], in which each copper cation is tetrahedrally coordinated by one 2-methylpyrazine and one trimethylphoshine ligand as well as two halide anions, are known. Similarly to the title compound, both copper cations are linked by two bridging halide anions into $(CuI)_2$ rings, but strikingly the binuclear units are linked by the 2-methylpyrazine ligands into chains. Moreover, $(CuI)_2$(2-methylpyrazine)$_2$-2-methylpyrazine solvate (XEBMEW; Rossenbeck & Sheldrick, 2000) also contains $(CuI)_2$ rings.

Finally, two compounds with the composition CuX(2-methylpyrazine)(triphenylphosphine)$_2$ with X = Cl, I [Refcodes: KAMKER (Ohara, *et al.*, 2017) and NAKYIL (Kondo *et al.*, 2020)] are reported, which form discrete complexes. This structural motif is unknown for compounds based on CuX and 2-chloropyrazine.

6. Synthesis and crystallization

Synthesis

CuI and 2-chloropyrazine were purchased from Sigma-Aldrich and used as received.

Yellow-colored single crystals suitable for single-crystal X-ray analysis were obtained within three days by the reaction of 0.5 mmol (95.23 mg) of CuI and 2 mL of 2-chloropyrazine. No stoichiometric ratios can be used as an excess of 2-chloropyrazine is needed because it acts as reactant and solvent. The additional 2-chloropyrazine cannot be removed by filtration and washing, because this leads immediately to the transformation of the title compound into CuI(2-chloropyrazine).

Experimental details

The data collection for single crystal structure analysis was performed using an Imaging Plate Diffraction System (IPDS-1) from Stoe with Mo $K\alpha$ radiation.

The PXRD measurements were performed with Cu $K\alpha_1$ radiation (λ = 1.540598 Å) using a Stoe Transmission Powder Diffraction System (STADI P) equipped with a MYTHEN 1K detector and a Johansson-type Ge(111) monochromator.

Differential thermoanalysis and thermogravimetry coupled to mass spectrometry (DTA–TG–MS) investigations were performed with a STA-429 thermobalance from Netzsch with skimmer coupling to a quadrupole mass spectrometer from Balzers. The measurements were performed in a dynamic nitrogen atmosphere in Al_2O_3 crucibles with a heating rate of 4°C min^{-1}. The instrument was calibrated using standard reference materials.

7. Refinement

Crystal data, data collection and structure refinement details are summarized in Table 3. The C—H hydrogen atoms were positioned in an idealized geometry and refined isotropically with $U_{iso}(H) = 1.2U_{eq}(C)$.

Table 3
Experimental details.

Crystal data	
Chemical formula	$[Cu_2I_2(C_4H_3ClN_2)_4]$
M_r	839.02
Crystal system, space group	Triclinic, $P\overline{1}$
Temperature (K)	220
a, b, c (Å)	7.5220 (6), 10.1067 (8), 10.1973 (9)
α, β, γ (°)	108.932 (9), 101.922 (10), 111.088 (9)
V (Å^3)	636.62 (11)
Z	1
Radiation type	Mo $K\alpha$
μ (mm^{-1})	4.54
Crystal size (mm)	0.25 × 0.20 × 0.18
Data collection	
Diffractometer	Stoe *IPDS1*
Absorption correction	Numerical (*X-SHAPE* and *X-RED 32*; Stoe, 2008)
T_{min}, T_{max}	0.556, 0.667
No. of measured, independent and observed [$I > 2\sigma(I)$] reflections	6865, 3018, 2670
R_{int}	0.041
Refinement	
$R[F^2 > 2\sigma(F^2)], wR(F^2), S$	0.037, 0.100, 1.02
No. of reflections	3018
No. of parameters	146
H-atom treatment	H-atom parameters constrained
$\Delta\rho_{max}, \Delta\rho_{min}$ (e Å^{-3})	1.22, −1.91

Computer programs: *X-AREA* (Stoe, 2008), *SHELXT2014/5* (Sheldrick, 2015*a*), *SHELXL2016/6* (Sheldrick, 2015*b*), *DIAMOND* (Brandenburg, 1999) and *publCIF* (Westrip, 2010).

Acknowledgements

Financial support by the State of Schleswig-Holstein is gratefully acknowledged.

References

Artem'ev, A. V., Beresin, A. S. & Bagryanskaya, I. Y. (2019). *J. Struct. Chem.* **60**, 967–971.

Brandenburg, K. (1999). *DIAMOND*. Crystal Impact GbR, Bonn, Germany.

Desiraju, G. R. & Sarma, J. P. (1986). *Proc. - Indian Acad. Sci. Chem. Sci.* **96**, 599–605.

Fitchett, C. M. & Steel, P. J. (2008). *Polyhedron*, **27**, 1527–1537.

Gibbons, S. K., Hughes, R. P., Glueck, D. S., Royappa, A. T., Rheingold, A. L., Arthur, R. B., Nicholas, A. D. & Patterson, H. H. (2017). *Inorg. Chem.* **56**, 12809–12820.

Groom, C. R., Bruno, I. J., Lightfoot, M. P. & Ward, S. C. (2016). *Acta Cryst.* B**72**, 171–179.

Herringer, S. N., Longendyke, A. J., Turnbull, M. M., Landee, C. P., Wikaira, J. L., Jameson, G. B. & Telfer, S. G. (2010). *Dalton Trans.* **39**, 2785–2797.

Hull, S. & Keen, D. A. (1994). *Phys. Rev. B*, **50**, 5868–5885.

Jana, S., Harms, K. & Chattopadhyay, S. (2016). *J. Iran. Chem. Soc.* **13**, 1713–1721.

Kondo, S., Yoshimura, N., Yoshida, M., Kobayashi, A. & Kato, M. (2020). *Dalton Trans.* **49**, 16946–16953.

Kromp, T. & Sheldrick, W. S. (1999). *Z. Naturforsch. B*, **54**, 1175–1180.

Kuwahara, T., Ohtsu, H. & Tsuge, K. (2020). *Inorg. Chem.* **60**, 1299–1304.

Li, D., Shi, W. J. & Hou, L. (2005). *Inorg. Chem.* **44**, 3907–3913.

Liu, W., Zhu, K., Teat, S. J., Deibert, B. J., Yuan, W. & Li, J. (2017). *Chem. Mater.* **5**, 5962–5969.

Mensah, A., Shao, J. J., Ni, J. L., Li, G. J., Wang, F. M. & Chen, L. Z. (2022). *Front. Chem.* **9**, 816363.

Näther, C., Bhosekar, G. & Jess, I. (2007). *Inorg. Chem.* **46**, 8079–8087.

Näther, C., Greve, J. & Jess, I. (2002). *Solid State Sci.* **4**, 813–820.

Näther, C. & Jess, I. (2001). *Monatsh. Chem.* **132**, 897–910.

Näther, C. & Jess, I. (2004). *Eur. J. Inorg. Chem.* pp. 2868–2876.

Näther, C., Jess, I. & Greve, J. (2001). *Polyhedron*, **20**, 1017–1022.

Näther, C., Jess, I., Lehnert, N. & Hinz-Hübner, D. (2003). *Solid State Sci.* **5**, 1343–1357.

Näther, C., Jess, I., Germann, L. S., Dinnebier, R. E., Braun, M. & Terraschke, H. (2017). *Eur. J. Inorg. Chem.* pp. 1245–1255.

Näther, C., Wriedt, M. & Jess, I. (2002). *Z. Anorg. Allg. Chem.* **628**, 394–400.

Ohara, H., Ogawa, T., Yoshida, M., Kobayashi, A. & Kato, M. (2017). *Dalton Trans.* **46**, 3755–3760.

Peng, R., Li, M. & Li, D. (2010). *Coord. Chem. Rev.* **254**, 1–18.

Rossenbeck, B. & Sheldrick, W. S. (1999). *Z. Naturforsch. B*, **54**, 1510–1516.

Rossenbeck, B. & Sheldrick, W. S. (2000). *Z. Naturforsch. B*, **55**, 467–472.

Sheldrick, G. M. (2015*a*). *Acta Cryst.* A**71**, 3–8.

Sheldrick, G. M. (2015*b*). *Acta Cryst.* C**71**, 3–8.

Stoe (2008). *X-AREA*, *X-RED32* and *X-SHAPE*. Stoe & Cie, Darmstadt, Germany.

Westrip, S. P. (2010). *J. Appl. Cryst.* **43**, 920–925.

supporting information

Acta Cryst. (2023). E**79**, 167-171 [https://doi.org/10.1107/S2056989023001238]

Synthesis, crystal structure and thermal properties of di-μ-iodido-bis[bis(2-chloropyrazine-κN)copper(I)]

Christian Näther and Inke Jess

Computing details

Data collection: *X-AREA* (Stoe, 2008); cell refinement: *X-AREA* (Stoe, 2008); data reduction: *X-AREA* (Stoe, 2008); program(s) used to solve structure: *SHELXT2014/5* (Sheldrick, 2015a); program(s) used to refine structure: *SHELXL2016/6* (Sheldrick, 2015b); molecular graphics: *DIAMOND* (Brandenburg, 1999); software used to prepare material for publication: *publCIF* (Westrip, 2010).

Di-μ-iodido-bis[bis(2-chloropyrazine-κN)copper(I)]

Crystal data

$[Cu_2I_2(C_4H_3ClN_2)_4]$
$M_r = 839.02$
Triclinic, $P\overline{1}$
$a = 7.5220$ (6) Å
$b = 10.1067$ (8) Å
$c = 10.1973$ (9) Å
$\alpha = 108.932$ (9)°
$\beta = 101.922$ (10)°
$\gamma = 111.088$ (9)°
$V = 636.62$ (11) Å^3

$Z = 1$
$F(000) = 396$
$D_x = 2.188$ Mg m^{-3}
Mo $K\alpha$ radiation, $\lambda = 0.71073$ Å
Cell parameters from 6865 reflections
$\theta = 2.5$–28.1°
$\mu = 4.54$ mm^{-1}
$T = 220$ K
Block, yellow
0.25 × 0.20 × 0.18 mm

Data collection

Stoe IPDS-1
diffractometer
Phi scans
Absorption correction: numerical
(X-Shape and X-Red 32; Stoe, 2008)
$T_{min} = 0.556$, $T_{max} = 0.667$
6865 measured reflections

3018 independent reflections
2670 reflections with $I > 2\sigma(I)$
$R_{int} = 0.041$
$\theta_{max} = 28.1°$, $\theta_{min} = 2.5°$
$h = -9 \rightarrow 9$
$k = -13 \rightarrow 13$
$l = -13 \rightarrow 13$

Refinement

Refinement on F^2
Least-squares matrix: full
$R[F^2 > 2\sigma(F^2)] = 0.037$
$wR(F^2) = 0.100$
$S = 1.01$
3018 reflections
146 parameters
0 restraints
Hydrogen site location: inferred from
neighbouring sites

H-atom parameters constrained
$w = 1/[\sigma^2(F_o^2) + (0.0731P)^2]$
where $P = (F_o^2 + 2F_c^2)/3$
$(\Delta/\sigma)_{max} = 0.001$
$\Delta\rho_{max} = 1.22$ e Å^{-3}
$\Delta\rho_{min} = -1.91$ e Å^{-3}
Extinction correction: *SHELXL2016/6*
(Sheldrick 2015b),
$Fc^* = kFc[1+0.001xFc^2\lambda^3/\sin(2\theta)]^{-1/4}$
Extinction coefficient: 0.043 (3)

Special details

Geometry. All esds (except the esd in the dihedral angle between two l.s. planes) are estimated using the full covariance matrix. The cell esds are taken into account individually in the estimation of esds in distances, angles and torsion angles; correlations between esds in cell parameters are only used when they are defined by crystal symmetry. An approximate (isotropic) treatment of cell esds is used for estimating esds involving l.s. planes.

Fractional atomic coordinates and isotropic or equivalent isotropic displacement parameters (Å²)

	x	*y*	*z*	$U_{\rm iso}$*/$U_{\rm eq}$
Cu1	0.83699 (6)	0.44607 (6)	0.88784 (5)	0.02577 (15)
I1	1.13274 (3)	0.38430 (3)	0.84123 (3)	0.02918 (13)
N1	0.1826 (5)	−0.0235 (4)	0.6635 (5)	0.0382 (8)
C1	0.2875 (6)	0.0483 (5)	0.8075 (5)	0.0310 (8)
C2	0.4784 (6)	0.1784 (5)	0.8761 (5)	0.0273 (7)
H2	0.545096	0.224589	0.980055	0.033*
N2	0.5673 (4)	0.2377 (4)	0.7947 (4)	0.0240 (6)
C3	0.4652 (6)	0.1671 (5)	0.6476 (5)	0.0352 (9)
H3	0.524713	0.206273	0.587078	0.042*
C4	0.2745 (7)	0.0380 (6)	0.5828 (5)	0.0400 (10)
H4	0.206856	−0.008357	0.478949	0.048*
Cl1	0.1760 (2)	−0.02696 (16)	0.91711 (16)	0.0573 (4)
N11	0.6729 (5)	0.7005 (4)	0.5844 (4)	0.0312 (7)
C11	0.5985 (6)	0.6885 (4)	0.6870 (4)	0.0271 (8)
C12	0.6478 (6)	0.6211 (5)	0.7776 (4)	0.0270 (7)
H12	0.589696	0.617235	0.850384	0.032*
N12	0.7785 (4)	0.5614 (4)	0.7617 (3)	0.0238 (6)
C13	0.8562 (5)	0.5723 (5)	0.6574 (4)	0.0267 (7)
H13	0.948559	0.531426	0.643161	0.032*
C14	0.8049 (6)	0.6421 (5)	0.5694 (5)	0.0311 (8)
H14	0.864111	0.648491	0.497602	0.037*
Cl11	0.42309 (19)	0.76067 (15)	0.70711 (14)	0.0455 (3)

Atomic displacement parameters (Å²)

	U^{11}	U^{22}	U^{33}	U^{12}	U^{13}	U^{23}
Cu1	0.0206 (2)	0.0312 (3)	0.0281 (3)	0.01328 (19)	0.00699 (17)	0.0157 (2)
I1	0.02846 (17)	0.03876 (19)	0.02799 (18)	0.02343 (12)	0.01185 (11)	0.01347 (12)
N1	0.0280 (16)	0.0314 (19)	0.043 (2)	0.0099 (14)	0.0061 (15)	0.0109 (16)
C1	0.0267 (17)	0.0208 (17)	0.043 (2)	0.0098 (14)	0.0161 (16)	0.0099 (16)
C2	0.0249 (17)	0.0229 (17)	0.0288 (19)	0.0099 (14)	0.0075 (14)	0.0080 (15)
N2	0.0185 (13)	0.0233 (15)	0.0279 (16)	0.0083 (11)	0.0045 (11)	0.0124 (13)
C3	0.0318 (19)	0.039 (2)	0.032 (2)	0.0127 (17)	0.0053 (16)	0.0214 (19)
C4	0.035 (2)	0.038 (2)	0.030 (2)	0.0087 (18)	−0.0033 (16)	0.0141 (19)
Cl1	0.0531 (7)	0.0426 (7)	0.0509 (7)	−0.0019 (5)	0.0312 (6)	0.0111 (6)
N11	0.0345 (17)	0.0280 (17)	0.0299 (17)	0.0132 (14)	0.0054 (13)	0.0166 (14)
C11	0.0267 (17)	0.0237 (17)	0.0264 (19)	0.0141 (14)	0.0013 (14)	0.0082 (15)
C12	0.0266 (17)	0.035 (2)	0.0263 (18)	0.0188 (15)	0.0113 (14)	0.0151 (16)
N12	0.0230 (14)	0.0247 (15)	0.0257 (15)	0.0123 (12)	0.0065 (11)	0.0135 (13)

C13	0.0230 (16)	0.0296 (19)	0.0288 (19)	0.0128 (14)	0.0079 (14)	0.0143 (16)
C14	0.0314 (18)	0.031 (2)	0.030 (2)	0.0118 (16)	0.0097 (15)	0.0162 (17)
Cl11	0.0526 (6)	0.0525 (7)	0.0470 (6)	0.0421 (6)	0.0143 (5)	0.0220 (5)

Geometric parameters (Å, º)

Cu1—N2	2.070 (3)	C3—H3	0.9400
Cu1—N12	2.078 (3)	C4—H4	0.9400
Cu1—Cu1^{i}	2.5643 (10)	N11—C11	1.302 (6)
Cu1—I1	2.6093 (5)	N11—C14	1.336 (6)
Cu1—I1^{i}	2.6476 (6)	C11—C12	1.380 (5)
N1—C1	1.313 (6)	C11—Cl11	1.739 (4)
N1—C4	1.342 (6)	C12—N12	1.336 (5)
C1—C2	1.382 (5)	C12—H12	0.9400
C1—Cl1	1.735 (4)	N12—C13	1.330 (5)
C2—N2	1.327 (5)	C13—C14	1.384 (6)
C2—H2	0.9400	C13—H13	0.9400
N2—C3	1.335 (5)	C14—H14	0.9400
C3—C4	1.378 (6)		
N2—Cu1—N12	103.01 (12)	N2—C3—H3	119.3
N2—Cu1—Cu1^{i}	130.55 (9)	C4—C3—H3	119.3
N12—Cu1—Cu1^{i}	126.35 (9)	N1—C4—C3	121.9 (4)
N2—Cu1—I1	109.42 (9)	N1—C4—H4	119.0
N12—Cu1—I1	107.83 (9)	C3—C4—H4	119.0
Cu1^{i}—Cu1—I1	61.554 (19)	C11—N11—C14	115.8 (3)
N2—Cu1—I1^{i}	107.58 (9)	N11—C11—C12	124.4 (4)
N12—Cu1—I1^{i}	105.80 (9)	N11—C11—Cl11	116.8 (3)
Cu1^{i}—Cu1—I1^{i}	60.06 (2)	C12—C11—Cl11	118.7 (3)
I1—Cu1—I1^{i}	121.61 (2)	N12—C12—C11	119.8 (3)
Cu1—I1—Cu1^{i}	58.39 (2)	N12—C12—H12	120.1
C1—N1—C4	115.1 (4)	C11—C12—H12	120.1
N1—C1—C2	124.4 (4)	C13—N12—C12	116.9 (3)
N1—C1—Cl1	117.0 (3)	C13—N12—Cu1	123.3 (3)
C2—C1—Cl1	118.6 (3)	C12—N12—Cu1	119.7 (3)
N2—C2—C1	119.7 (4)	N12—C13—C14	121.8 (4)
N2—C2—H2	120.1	N12—C13—H13	119.1
C1—C2—H2	120.1	C14—C13—H13	119.1
C2—N2—C3	117.4 (3)	N11—C14—C13	121.3 (4)
C2—N2—Cu1	122.7 (3)	N11—C14—H14	119.3
C3—N2—Cu1	119.5 (3)	C13—C14—H14	119.3
N2—C3—C4	121.4 (4)		

Symmetry code: (i) $-x+2, -y+1, -z+2$.

Hydrogen-bond geometry (Å, º)

D—H···*A*	*D*—H	H···*A*	*D*···*A*	*D*—H···*A*
C3—H3···N11^{ii}	0.94	2.68	3.241 (5)	119

C13—H13···I1	0.94	3.24	3.872 (4)	127

Symmetry code: (ii) $-x+1$, $-y+1$, $-z+1$.